RESEARCH ARTICLE | APRIL 10 2019

The mechanical role of a cytoskeletal protein, Synemin, in bone, heart and skeletal muscle FREE

Karla P. García-Pelagio; Atum M. Buo; Ling Chen; Megan Moorer; Joseph P. Stains; Robert J. Bloch

AIP Conf. Proc. 2090, 050008 (2019)
https://doi.org/10.1063/1.5095923

The Mechanical Role of a Cytoskeletal Protein, Synemin, in Bone, Heart and Skeletal Muscle

Karla P. García-Pelagio[1,2a], Atum M. Buo[3,b], Ling Chen[2,c], Megan Moorer[3,d], Joseph P. Stains[3,e], Robert J. Bloch[2,f]

[1]*Departmento de Física, Facultad de Ciencias,Universidad Nacional Autonoma de Mexico, Av Univerisidad 3000 UNAM, Mexico City, 04360, Mexico*

[2]*Department of Physiology, School of Medicine, University of Maryland, 655 W Baltimore St, Baltimore, MD 21201, USA*

[3]*Department of Orthopaedics, School of Medicine, University of Maryland, 655 W Baltimore St, Baltimore, MD 21201, USA*

[a] *kpaolag@ciencias.unam.mx*,
[b] *abuo001@umaryland.edu,*
[c] *lchen685@gmail.com*,
[d] *moorer.megan@gmail.com,*
[e] *jstains@som.umaryland.edu,*
[f] *rbloch@som.umaryland.edu*

Abstract. Intermediate filaments (IFs) represent a major cytoskeletal network contributing to force transmission, cell shape and structure, adhesion and motility, subcellular scaffolding and tissue resilience, thereby modulating a range of cellular activities. Life-threatening disorders associated with IF mutations have pushed investigations to study IFs of mammalian cells in culture and *in vivo*. Keratin and Lamin related disorders, Desmin-related myopathy, Muscular Dystrophies, Alexander disease are just examples of pathologies related to IFs. Synemin, a type IV IF has become a target for research since its AKAP role in the heart was reported. Here we summarize our results with Synemin "knock-out" mice showing that Synemin plays a significant role in skeletal and cardiac muscle, leading to a mild skeletal myopathy and a mixed cardiomyopathy. We also report an important role of Synemin, with the absence of Synemin leading to osteopenia.

INTRODUCTION

Intermediate Filaments (IFs) are structural proteins of the nuclear membrane and the cytosol that determine cellular architecture and cytoplasmic integrity (1, 2, 3). IFs also serve as a scaffold for enzymes involved in intracellular signaling (3, 4) and in directing the assembly of microtubules (5), thereby modulating a range of cellular activities, including motility (1). IFs are key components of costameres, structures that align the cell membrane regularly with nearby myofibrils and transmit contractile force laterally from myofibrils to the extra-cellular matrix [6,7].There are more than 65 different genes coding for IF proteins of 6 different classes (8,9). These include the keratins (types I and II); desmin, vimentin and glial fibrillar acidic protein (type III); neurofilament proteins, internexin and synemin (type IV); the nuclear lamins (type V); and other, tissue-specific filament proteins, such as phakinin, filensin, and nexin (type VI). A large number of human diseases ranging from skin disorders [10] to skeletal and cardiac myopathy [11,12,13], as well as premature aging, are caused by mutations in genes encoding specific intermediate filament (IF) proteins. The type IV intermediate filament protein, synemin, coassembles into desmin or vimentin filaments and can associate with keratin filaments it also serves as an A-kinase anchoring protein (AKAP) (Figure 1). Synemin is encoded by a single gene (*Synm*) and is primarily expressed as either α or β isoforms, with molecular masses of 220 and 180 kDa, respectively. We have been studying the roles of IFs in striated muscle, and report that it provides a passive mechanical scaffold to maintain cytoplasmic integrity and facilitate lateral transmission of contractile force [14, 15, 16, 17]. Like striated muscle, bone is of mesenchymal origin and expresses keratins and vimentin. Here we report that mice lacking synemin (*Synm*-/-, *Synm*-null) are also osteopenic, with a more than 50% reduction in trabecular bone density (18).

XV Mexican Symposium on Medical Physics
AIP Conf. Proc. 2090, 050008-1–050008-6; https://doi.org/10.1063/1.5095923
Published by AIP Publishing. 978-0-7354-1820-2/$30.00

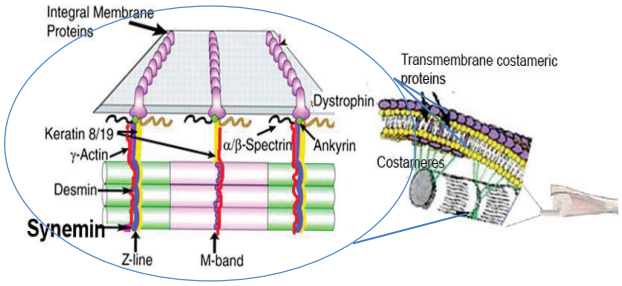

FIGURE 1. IFs in skeletal muscle. IFs surround the contractile apparatus and link Z line proteins to the cell membrane at costameres stabilizing the cell membrane.

MATERIALS AND METHODS

Animals. Phenotyping of skeletal muscle and bone were performed in male *Synm* -/- mice of 3 mo of age while cardiac muscle experiments were carried out with male mice at 3 and 15 mo of age. C57Bl/6 mice of the same ages served as controls (WT). Animals were anesthetized with isofluorane (2% with oxygen, 0.5 l/min) and euthanized by cervical dislocation. All of our protocols were approved by the Institutional Animal Care Committee of the University of Maryland, School of Medicine.

For bone experiments:

X-ray imaging. Post euthanasia, lateral and AP radiographs (35 kV, 10 s) were taken of the mice using a Faxitron digital X-ray system, as described (18).

MicroCT. Femurs were dissected from WT and *Synm* -/- mice, fixed in 4% paraformaldehyde for up to 4 days and then transferred to 70% ethanol. Three-dimensional microCT was performed on the femurs of 7 animals for gross morphological assessment using a Bruker SkyScan 1172 microCT scanner. Bone microarchitecture were assessed at the distal femoral metaphysis for trabecular parameters such as: ratio of bone and tissue volume (BV/TV), trabecular number (Tb.N), trabecular thickness (Tb.Th.), and trabecular separation (TbSp). For cortical parameters were measured: periosteal perimeter (Ps.Pm), endocortical perimeter (Ec.Pm), cortical cross sectional thickness (Cs.Th) and mean polar moment of inertia (MMI).

For heart muscle experiments:

Echocardiography. Left ventricle images were obtained using a transthoracic M-mode echocardiography high-resolution ultrasound (Vevo 2100, Fiji-VisualSonics, Toronto, ON, Canada) equipped with a 40-MHz scanhead.

Left ventricular pressure-volume (PV) loop analysis. Animals were orally intubated and ventilated via a rodent ventilator (Model 683, Harvard Instruments, Holliston, MA). After 10-15 min stabilization the loop data were recorded using an ADVantage System (ADV500, Transonic-Science). Data were analyzed offline with LabChart Pro (Version 8.1.5, ADInstruments, Sydney, Australia).

Hematoxylin and eosin staining. Frozen cross sections were fixed with cold acetone, air dried, immersed in Harris hematoxylin (Sigma-Aldrich, St. Louis, MO), then in Scotts Bluing reagent (ThermoFisher Scientific), followed by Eosin staining, with rinsing steps of tap water between solution changes, and finally through a gradient of increasing concentrations of ethanol, as previously described [25]. The sections were observed under light microscopy (Zeiss Axioscope, x20 objective and x2 eyepiece), and representative digital images were captured.

Masson trichrome staining. Frozen cross sections were fixed with cold acetone, air dried, immersed in Bouin´s solution, then in Weigert´s Iron Hematoxylin, followed by Biebrich Scarlet-Acid Fuchsin, phosphotungstic / phosphomolybdic acid, and then with Aniline Blue. The sections were observed under light microscopy (Zeiss Axioscope, x20 objective and x2 eyepiece), and representative digital images were captured.

For skeletal muscle experiments:

Biomechanical properties. We used an elastimeter, which we described in detailed before [18, 19]. We determine a set of mechanical properties such as: bleb displacement as a function of pressure, pressure at which the cell membrane separates from nearby myofibrils, stabilization time of the membrane under constant pressure, and the pressure at which the sarcolemma bursts. Photomicrographs of the bleb were taken with a 10.2 Mpix digital camera (SONY α-

70, Sony Corporation, Tokyo, Japan) through a x10 eyepiece and x40, N.A. 0.75 water immersion objective and then analyzed with Image J software (NIH, Bethesda, MD).

Muscle injury. Anesthetized mice were placed in a supine position, with its hindlimb stabilized and the foot secured onto a plate linked to a stepper motor and torque sensor as previously described (20). The anterior muscles of the lower hindlimb were tetanically stimulated via the peroneal nerve, and 200 ms later the foot was forced into plantarflexion through a 90° arc of motion (–10° to 80°, with the foot orthogonal to the tibia considered as 0°) at an angular velocity of 900°/s. The stimulation and forced plantarflexion were repeated 15 times over a period of 15 min. This procedure induces injury to large-strain lengthening contractions.

RESULTS

Osteopenia is observed in Synemin KO Mice

At 3 mo old, *Synm -/-* and WT (*Syn +/+)* mice were almost indistinguishable except for body weight (Fig 2A,B). While there is a slight decrease in body weight in *Synm -/-* mice relative to controls, there is no significant difference in body length (nose to tip of the tail) or tibia length (Fig 2B).

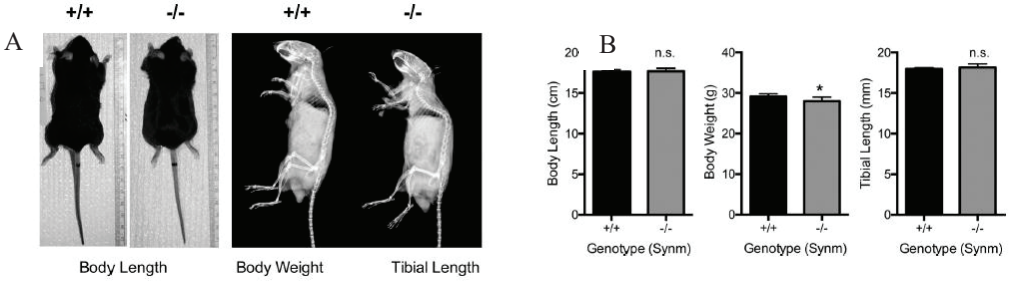

FIGURE 2. (A) *Synm*-null mice appear grossly normal relative to control mice. (B) Body length, weight and tibia length is shown in the graphs.

Studies in microCT show that *Synm -/-* mice are severely osteopenic, with a more than two-fold decrease in trabecular bone mass (BV/TV) relative to WT controls (Fig. 3A,B). Likewise, a subtle cortical bone phenotype was observed at the femoral middiaphysis, including a reduced cross-sectional area of the diaphysis due to an attendant reduction in both the periosteal and endosteal perimeter (Fig. 3C).

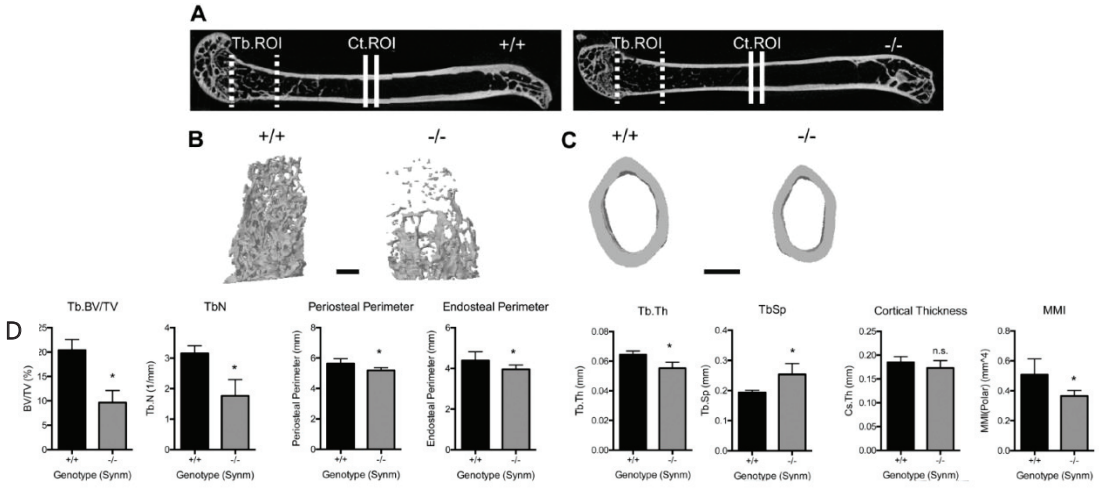

FIGURE 3. *Synm*-null mice have a trabecular and cortical bone phenotype. (A) Longitudinal digital X-ray of the femur. (B) *Synm*-null mice are shown for trabecular bone at the metaphysis of the distal femur or (C) Cortical bone at the femoral middiaphysis. (D) Bone microarchitecture parameters for trabecular and cortical bone.

This evidence points to a critical role for Synemin in bone, such that its absence leads to severe osteopenia (18).

Mixed Cardiomyopathy is present in Synemin null mice

We studied the hearts of *Synm* −/− mice in vivo to assess the role of synemin in the structure and function of cardiac muscle in mice at young and older ages. We used echocardiography as a non-invasive method to evaluate changes of LV geometry and function in WT and *Synm* −/− mice at young and older ages (Fig 4A-D). We next performed PV loop analysis to evaluate LV performance, as it is less confounded by loading conditions than echocardiography (Fig 4E-H).

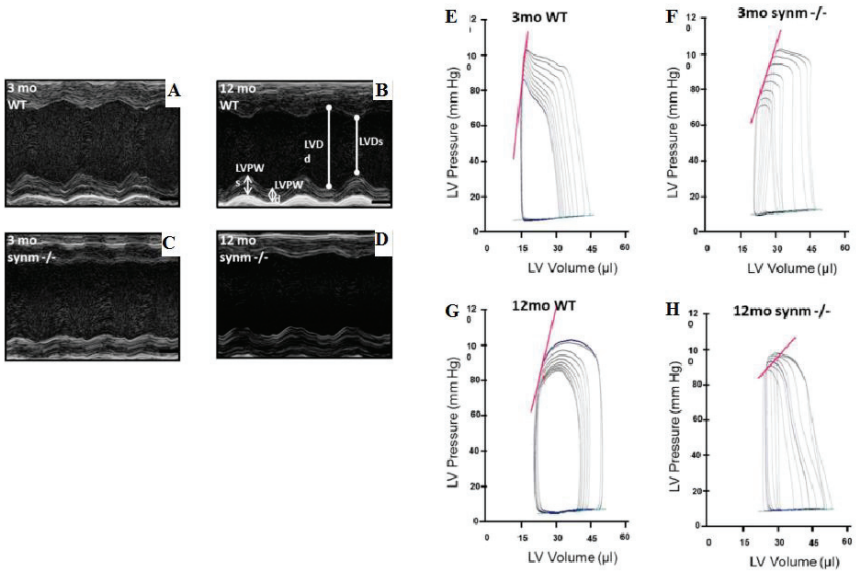

FIGURE 4. Echocardiographic (A-D) and P-V loop results in *Synm*-null mice at young and old ages (E-H).

We found morphological changes related to the synemin absence (Fig. 5).

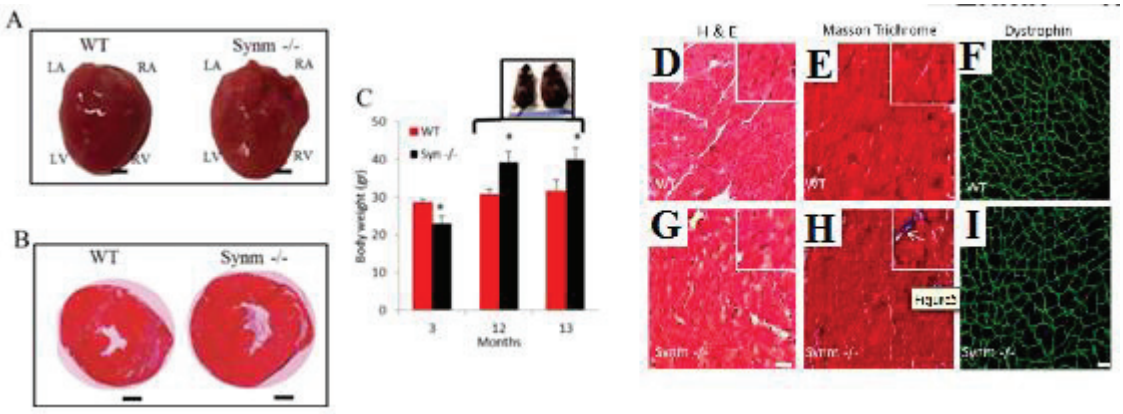

FIGURE 5. Heart phenotype in *Synm* −/− mice. (A) Frozen heart and (B)cross sections of *Synm* −/− and WT heart stained with hematoxylin and eosin. (C) Body weight (BW), and body and heart weight (HW) normalized to tibia length (TL). Cross heart sections stained with H&E (D,G), Mason Trichrome (E,H) and dystrophin (F,I). Bars indicate means SD; **P* <0.05.

This result show that synemin plays a physiologically significant role in cardiac muscle, and its absence leads to physiological changes associated with cardiomyopathy (19).

Changes in skeletal muscle denote a mild muscular dystrophy

We studied fast-twitch muscles from *Synm -/-* mice to assess the role of this IF protein in muscle structure and function. We assessed the elastic properties of the sarcolemmal membrane and the strength of its connections to the underlying contractile apparatus by Elastimetry (Fig 6A-D).

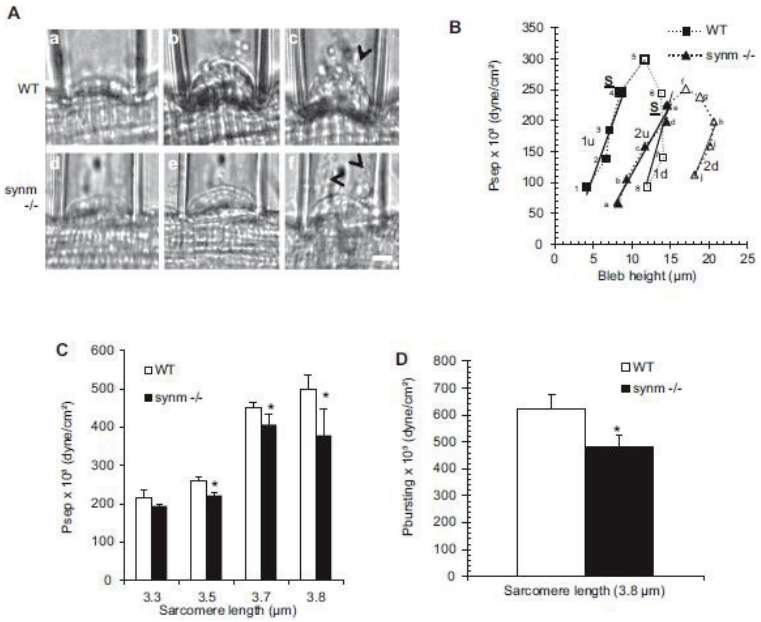

FIGURE 6. Biomechanical properties of the surface of single control and *Synm -/-* extensor digitorum longus (EDL) fibers measured by Elastimetry in vitro. (A) Representative photographs of blebs formed with progressively increasing pressures. (B) Pressure-displacement curve in control and *Synm -/-* myofibers. (C) Effect of sarcomere length on separation pressure. (D) Histogram of bursting pressure. Bars indicate means SD; **P* <0.05.

We assessed the contribution of synemin to the function of muscle tissue by measuring maximal isometric contractile force produced by the TA muscles in anesthetized animals.

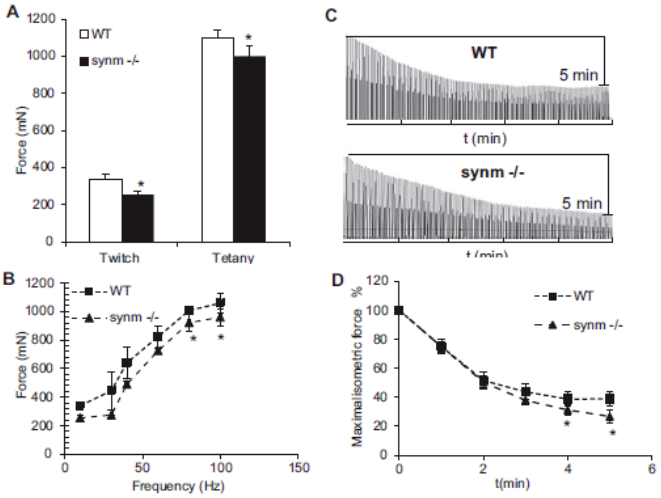

FIGURE 7.Measurements of contractile force and fatigability. *(A)* Single twitch and maximal tetanic force of TA muscles were measured in situ. (*B)* Force-frequency relationship. (C) Representative trace recordings of fatigue. (D) Rate of muscle fatigue in situ at maximal isometric force. For WT and *Synm*-null mice.

Thus synemin plays a moderate but distinct role in fast twitch skeletal muscle such that its absence leads to a mild skeletal myopathy (17).

DISCUSSION

We report that genetic ablation of Synemin in mice results in abnormalities in bone, as well as in skeletal and cardiac muscle. We found osteopenia with reduction in trabecular and cortical bone fraction. Skeletal muscle in null mice have a mild phenotype denoted by decreased fiber size and force production, and increased sarcolemmal deformability and susceptibility to injury. In the heart, the absence of synemin causes left ventricular systolic dysfunction associated with hypertrophy and dilatation. Thus, synemin plays important roles in bone (18), cardiac (19) and skeletal muscles (17).

ACKNOWLEDGMENTS

This work was supported partially by Grants R01-AR-063631 (J. P. Stains) and R01-AR-055928 (R. J. Bloch) from the NIH, and UNAM-PAPIIT IA207818 (K.P.Garcia-Pelagio).

REFERENCES

1. Li Z, Colucci-Guyon E, Pincon-Raymond M, Mericshay M, Pourin S, Paulin D, and Babinet C. Dev. Bio. **175**, 362–366 (1996)
2. Herrmann H, Strelkov SV, Burkhard P and Aebi U. J. Clin. Invest. **119**, 1772–1783 (2009).
3. Dalakas M, Park KY, Semino-Mora C, Lee HS, Sivakumar K, and Goldfarb L. N Engl J Med **342**, 770-780 (2000)
4. Goldman R, Khuon S, Chou Y, Opal P and Steinert P. J Cell Biol **134**, 971-983 (1996)
5. Herrmann H, Bar H, Kreplak L, Strelkov SV and Aebi U. Nat Rev Mol Cell Biol **8**(7), 562-73 (2007)
6. Garcia-Pelagio K, Bloch R, Ortega A, Gonzalez-Serratos H AIP Conf Proc **854**, 51–53 (2006).
7. Bloch R, Gonzales-Serratos H. Exerc Sport Sci Rev 31(2), 73–78, (2004)
8. Helfand B, Chang L and Goldman R. J Cell Sc **117**, 133-141 (2004)
9. Paramio J and Jorcano L. Bioassays **24** (9), 836-44 (2002)
10. Lazarides, E. Nature **283**, 249- 256 (1980)
11. Capetanaki Y, Bloch RJ, Kouloumenta A, Mavroidis M and Psarras S. Exp Cell Res **313**(10), 2063-76 (2007)
12. Pardo JV, Siliciano J and Craig S. Proc. Natl. Acad. Sci. **80**, 1008-1012 (1983)
13. Bloch RJ, Capetanaki Y, O´Neill A, Reed P, Williams M, Resneck W, Porter N and Ursitti J. Clin Orthop Relat Res **403**, S203-S210 (2002)
14. Lund M, Kerr J, Lupinetti J, Zhang Y, Russell M, Bloch R and Bond M. FASEB **1**, 137-148 (2011)
15. Sun N, Critchley D, Paulin D, Li Z and Robson R. Exp. Cell. Res. **314**, 1839-1849 (2008)
16. Ursitti J, Lee P, Resneck W, Mc Nally M, Bowmann A, O´Neill A, Stone M and Bloch RJ. J Biol Chem **270**(40), 41830-41838 (2004)
17. García-Pelagio K, Muriel J, O´Neill A, Desmond P, Lovering R, Lund L, Bond M, Bloch R. Am J Physiol Cell Physiol; **308**(6), C448-62 (2015)
18. Moorer M, Buo A, García-Pelagio K, Stains J, Bloch R. Am J Cell Physiol **11**(6), C839-C845 (2016)
19. Garcia-Pelagio KP, Chen L, Joca H, Ward C, Lederer J, Bloch R. J Mol Cell Cardiol **114**, 354-363 (2018)